

Representation of Linear Terrain Features in a 2D Flood Model with Regular Cartesian Mesh

Mustafa Altinakar¹, Marcus McGrath², Yavuz Ozeren³, and Edie Miglio⁴

¹NCCHE, The University of Mississippi. Carrier Hall, Room 102, P.O. Box 1848, University, MS, 38677-1848; PH (662) 915-3783; FAX (662) 915-7796; email: altinakar@ncche.olemiss.edu

²NCCHE, The University of Mississippi. Carrier Hall, Room 102, P.O. Box 1848, University, MS, 38677-1848; PH (662) 915-3960; FAX (662) 915-7796; email: mzmcgrat@ncche.olemiss.edu

³NCCHE, The University of Mississippi. Carrier Hall, Room 102, P.O. Box 1848, University, MS, 38677-1848; PH (662) 915-6559; FAX (662) 915-7796; email: hhomari@ncche.olemiss.edu

⁴MOX, Dept. of Mathematics "F. Brioschi", Politecnico di Milano. Piazza Leonardo da Vinci, 32, 20133 Milano, Italy; PH +39-02-239 94 600; FAX +39-02-239 94 606, email: edie.miglio@polimi.it (visiting scientist at NCCHE during 2007)

ABSTRACT

Highly transient floods resulting from the failure of dams and levees can lead to loss of life and property damage. Two-dimensional (2D) numerical simulations that use modern shock-capturing schemes are particularly suited to simulate these mixed-regime floods for flood mapping, consequence analysis and emergency management planning. The Digital Elevation Models (DEM) are often used as a regular computational mesh. Unfortunately, linear terrain features, such as road and railroad embankments and dikes, which may influence flood patterns, are not adequately captured in DEMs. This study describes a two-sided cut-cell boundary method for representing linear terrain features on a regular Cartesian mesh. The proposed method is briefly described and some test simulations are presented.

INTRODUCTION

Dams and levees are one of the eighteen critical infrastructures/key- resource sectors that require protective actions to prepare for, or to mitigate against, a terrorist attack or other hazards. Their failure leads to highly transient flows that can cause loss-of-life, property damage and cascading failures in other critical sectors.

US National Inventory of Dams (NID, 2008) currently lists about 79,000 dams in the USA, including those in Guam and Puerto Rico. Only about 5% of these dams are owned by the federal government. The majority of the remaining dams are privately owned and they are under the responsibility of the states. Out of the 79,000 existing dams, 11,243 are classified as high hazard and 12,656 as significant hazard dams. All high hazard dams are required to have an Emergency Action Plan (EAP) identifying potential emergency conditions at a dam and specifying preplanned actions to be followed to minimize property damage and loss of life. The EAP also contains inundation maps and the procedures and information to assist the dam owner/operator in issuing early warning and notification messages to responsible downstream emergency management authorities. Unfortunately, 5,035 high hazard dams and 6,013 significant hazard dams do not yet have an EAP. Among these, 1,858 high-hazard dams and 2,533 significant hazard dams were built before 1940.

Two-dimensional (2D) numerical models based on modern conservative shock-capturing schemes can provide a cost effective way to prepare EAPs for all high-hazard and significant-hazard dams. The 2D numerical models can directly use Digital Elevation Maps (DEM), which are readily available from federal and state owned geospatial data clearinghouses. This greatly facilitates input data preparation. The 2D simulation captures the highly dynamic nature of these floods and provides reliable results even in flat areas without channelized flow. Moreover, simulation results can be readily imported into a GIS platform, as raster or shape files, to be used for map creation, risk and vulnerability analyses, and flood emergency management and decision support.

Using a DEM directly as computational mesh, however, presents certain drawbacks. For typical DEM resolutions of 30m to 100m used in dam-break studies, the DEMs do not adequately capture linear terrain features, such as road and railroad embankments, which may constitute obstacles and influence the flood propagation and inundation limits. Increasing the resolution or using a locally refined unstructured triangular mesh is not always desirable as it may lead to longer computational times due to CFL (Courant-Friedrichs-Lewy) condition.

The present paper discusses the implementation of a two-sided cut-cell boundary method (or immersed boundary method) in a 2D numerical model in order to represent linear terrain features on a regular Cartesian mesh without penalizing the time step. A few test cases are also presented.

DESCRIPTION OF THE NUMERICAL MODEL CCHE2D-FLOOD

Consider the two-dimensional shallow water flow depicted in Figure 1. Two-dimensional unsteady shallow water equations governing the flood flow can be written in the following vector form:

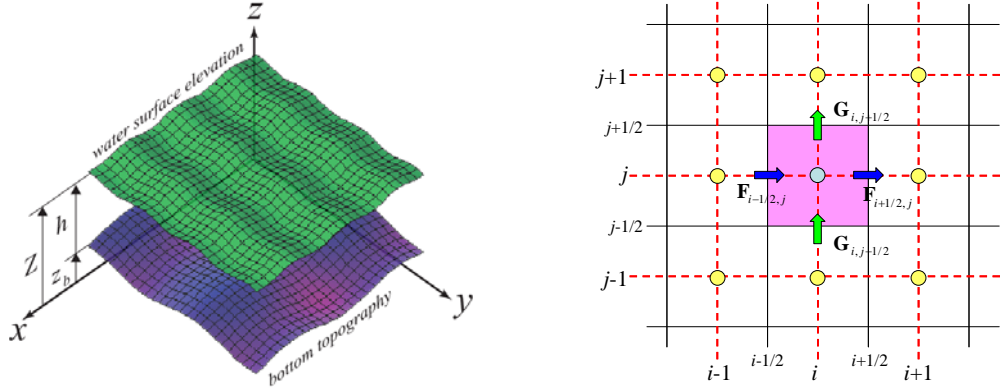


Figure 1. Left: Definition sketch for a two-dimensional shallow water flow; Right: Regular Cartesian computational grid.

$$\frac{\partial \mathbf{U}}{\partial t} + \frac{\partial \mathbf{F}(\mathbf{U})}{\partial x} + \frac{\partial \mathbf{G}(\mathbf{U})}{\partial y} = \mathbf{S}(\mathbf{U}) \quad (1)$$

where \mathbf{U} is the vector of conserved variables; $\mathbf{F}(\mathbf{U})$ and $\mathbf{G}(\mathbf{U})$ are the flux vectors in horizontal x and y directions:

$$\mathbf{U} = \begin{bmatrix} h \\ hu \\ hv \end{bmatrix} = \begin{bmatrix} h \\ Q_x \\ Q_y \end{bmatrix} \quad ; \quad \mathbf{F} = \begin{bmatrix} Q_x \\ Q_x^2 / h \\ Q_x Q_y / h \end{bmatrix} \quad ; \quad \mathbf{G} = \begin{bmatrix} Q_y \\ Q_y Q_x / h \\ Q_y^2 / h \end{bmatrix} \quad (2)$$

In the above equations, h is the water depth, u and v are the components of horizontal velocity vector in x and y directions. The components of volume flux (discharge) in x and y directions are represented by Q_x and Q_y . The vector of source terms $\mathbf{S}(\mathbf{U})$ is given by:

$$\mathbf{S} = \begin{bmatrix} q_v \\ -gh(\partial Z / \partial x) - g \left(u \sqrt{u^2 + v^2} / C^2 \right) \\ -gh(\partial Z / \partial y) - g \left(v \sqrt{u^2 + v^2} / C^2 \right) \end{bmatrix} \quad (3)$$

where q_v is a volume source or sink located in the cell, Z is the water surface elevation with respect to the reference plane and C the Chezy friction coefficient.

Referring to the computational grid represented in Figure 1, cell-centered finite-volume discretization of Eq. 1 over a rectangular control volume leads to the following explicit scheme:

$$U_{ij}^{n+1} = U_{ij}^n - \frac{\Delta t}{\Delta x_i} (F_{i+1/2,j} - F_{i-1/2,j}) - \frac{\Delta t}{\Delta y_j} (G_{i,j+1/2} - G_{i,j-1/2}) + \Delta t S_{ij} \quad (4)$$

where Δx and Δy represent the cell dimensions in x and y directions, and Δt is the time step. The terms $F_{i+1/2,j}$, $F_{i-1/2,j}$, $G_{i,j+1/2}$ and $G_{i,j-1/2}$ represent the *intercell*

fluxes along the four cell edges. The two-dimensional (2D) numerical model CCHE2D-FLOOD, which was developed at the National Center for Computational Hydroscience and Engineering of the University of Mississippi, uses the first order upwinding method to compute the intercell fluxes:

$$\mathbf{F}_{i+1/2j} = \begin{bmatrix} Q_x \\ Q_x^2/h \\ Q_x Q_y/h \end{bmatrix}_{i+k} \quad k = \begin{cases} 0 & Q_x \geq 0 \\ 1 & Q_x \leq 0 \end{cases}; \quad \mathbf{G}_{ij+1/2} = \begin{bmatrix} Q_y \\ Q_y Q_x/h \\ Q_y^2/h \end{bmatrix}_{j+m} \quad m = \begin{cases} 0 & Q_y \geq 0 \\ 1 & Q_y \leq 0 \end{cases} \quad (5)$$

The above upwinding relationships for intercell fluxes are supplemented by additional relationships to take into account special conditions, such as wet and dry cell interactions, converging flows, very steep ground elevations, etc. The source terms are discretized in the following manner:

$$\mathbf{S} = \begin{bmatrix} q_v \\ -gh_{ij}^{n+1} \left[\left(\frac{\partial Z}{\partial x} \right) \right] - g \left(\frac{u_{ij} \sqrt{u_{ij}^2 + v_{ij}^2}}{(h_{ij}^{1/6}/n)^2} \right) \\ -gh_{ij}^{n+1} \left[\left(\frac{\partial Z}{\partial y} \right) \right] - g \left(\frac{v_{ij} \sqrt{u_{ij}^2 + v_{ij}^2}}{(h_{ij}^{1/6}/n)^2} \right) \end{bmatrix} \quad \text{with} \quad C = \frac{h_{ij}^{1/6}}{n} \quad (6)$$

where n represents the Manning's roughness coefficient.

The CCHE2D-FLOOD model handles dry-bed condition by maintaining a very small water depth, which is chosen sufficiently small not to cause any noticeable change in the propagation speed of the wet/dry front. When a wet cell and dry cell share a common edge, only the mass flux is allowed into the dry cell (momentum flux is set to zero) during that particular time step.

The numerical code resulting from this discretization is stable, robust and oscillation-free near discontinuities. It has been shown to rigorously conserve mass and momentum. No special entropy fixes are needed to ensure physically plausible solutions. CCHE2D-FLOOD has been verified and validated using analytical solutions as well as data from laboratory experiments, model tests, and past dam break events (see Ying et al., 2003a and b; Ying and Wang, 2004; and Ying et al., 2004).

Different types of boundary conditions are implemented in CCHE2D-FLOOD: 1) fully reflecting impervious solid boundary; 2) open boundary (which allows the flow to exit the computational domain freely); 3) stage-time boundary (which allows to specify the water surface elevation at the boundary as a function of time); 4) inlet boundary (which allows definition of a discharge hydrograph entering or leaving through the boundary).

CCHE2D-FLOOD uses an explicit scheme to solve the shallow water equations. It is, therefore, subjected to the Courant-Friedrichs-Lewy (CFL) condition for stability and convergence. Given a mesh size, $\Delta x \times \Delta y$, the CFL condition places an upper bound on the time step as follows:

$$N_{CFL} = \text{Max} \left[\frac{\Delta t}{\Delta x} (|u| + \sqrt{gh}), \frac{\Delta t}{\Delta y} (|v| + \sqrt{gh}) \right] \leq 1 \quad (7)$$

The time step can be either automatically selected by the program based on the consideration of the CFL condition or directly specified by the user.

CUT-CELL BOUNDARY METHOD AND LINEAR TERRAIN FEATURES

A two-sided cut-cell boundary (or immersed boundary) method was implemented in CCHE2D-FLOOD to represent linear terrain features on a regular rectangular Cartesian mesh. Referring to Figure 2, the linear terrain feature to be represented in the 2D model is projected onto the DEM from a GIS shape layer by imposing the following rules: 1) a cell can only be cut by a single straight line; 2) The line joining the centers of two adjacent cells can only be cut by a single straight cut-line, 3) When two adjacent cells are both cut by a line, the cut lines should meet at the same point on the common edge. The projected line cuts through computational cells and divides them into two irregular-shaped parts. Some of the irregular-shaped cells can be very small. The main challenge resides in developing a scheme that does not require smaller time steps to meet the CFL condition for stability. The oscillation-free shock-capturing property of the scheme must also be preserved.

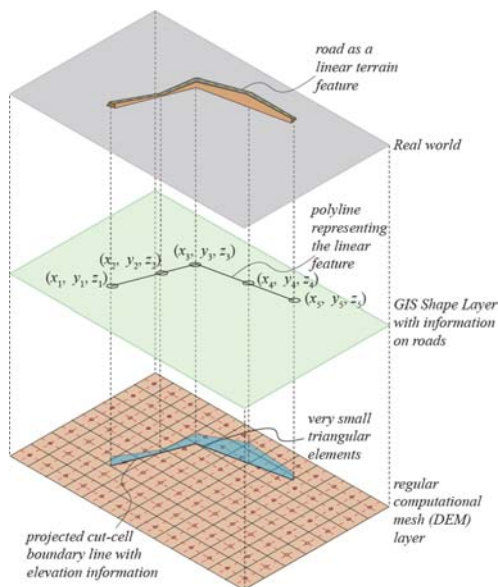


Figure 2. Projection of a linear terrain feature on the regular Cartesian Mesh.

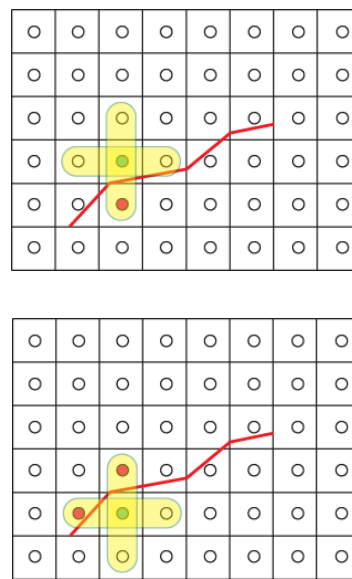


Figure 3. Computational stencils in the presence of a cut-cell boundary.

Several methods have been proposed to deal with cut-cells in two and three-dimensional meshes. Causon et al. (2000) combines cut-cells with adjoining regular cells to avoid small time steps. The h-box method (Helzel et al., 2005) use a rotated control volume for calculating the flux through the cut-cell boundary. The present study has adopted the Ghost Fluid Method (GFM) (Ghias et al., 2007), which is a special form of a class of techniques called Immersed Boundary Method (IBM) (Mittal and Iaccarino, 2005). The two-sided version of GFM implemented in CCHE2D-FLOOD is described in Miglio et al. (2008). Here only a brief presentation of the method will be given and some test cases will be presented.

Figure 3 shows the computational stencil in the presence of a cut-cell boundary. In the upper figure, the computed point (shaded green) is located in the upper side of the cut line representing the linear terrain feature. The cell below (shaded red) lies on the other side of the boundary; thus, the variables at the cell center are not available for applying the stencil. When calculating the cell below the cut line, the values of variables for cells above and on the left are not available for applying the stencil. The missing cells of the computational stencil are said to be *ghost cells* (GP) with respect to the cell being computed. The idea behind the GFM method is to use specially computed values for the variables in ghost cells in such a way that the following boundary conditions are enforced along the cut-line:

$$Q_n = q, \quad \frac{dQ_t}{dn} = 0, \quad \frac{dZ}{dn} = 0, \quad (8)$$

where Q_n and Q_t are the normal and the tangential components of the discharge, Z the water surface elevation, $\mathbf{n} = [n_x, n_y]$ the vector normal to the immersed boundary and q represents the overtopping discharge, if any, which can be calculated using an appropriate weir equation, for example.

The computational procedure to determine the values of the variables in ghost cells will be explained referring to Figure 4. In both left and right cases, the cell (i, j) is being computed. In the left hand side configuration, the cell $(i, j - 1)$ is a ghost point (GP) with respect to the computed cell (i, j) . To compute the flux across the lower edge, the values of the unknown must be defined at GP in such a way that the boundary conditions along the immersed boundary are correctly represented. To find the unknown values at GP, the point GP is first reflected onto the other side of the immersed boundary to find the *reflected point* RP. Note that the line segments $GP - B_{34}$ and $B_{34} - RP$ have the same length. The value at RP can be calculated by bilinear interpolation using the known values of the variables at the surrounding cells.

The values at GP are then linearly extrapolated from RP using the boundary conditions at B (Eq. 8). Once the values to be used at GP are determined, the computational stencil can be directly applied to compute the next step values for the cell (i, j) . This was the simplest situation where all the four corner nodes of the

interpolation cell are on the same side of the cut-cell boundary as the computed cell. A different situation arises when all the corners of the interpolation cell are not on the same side as the computed cell. Such a case is depicted on the right hand side of Figure 4. The corner 1 of the interpolation cell is on the opposite side of the cut-cell boundary and, thus, its value is not defined. The fix in such cases is to replace the missing corner by the boundary condition; in this case condition at B_{34} . The rest of the procedure basically remains the same. Details of the method and derivation of the equations for different situations are presented in detail in Miglio et al. (2000).

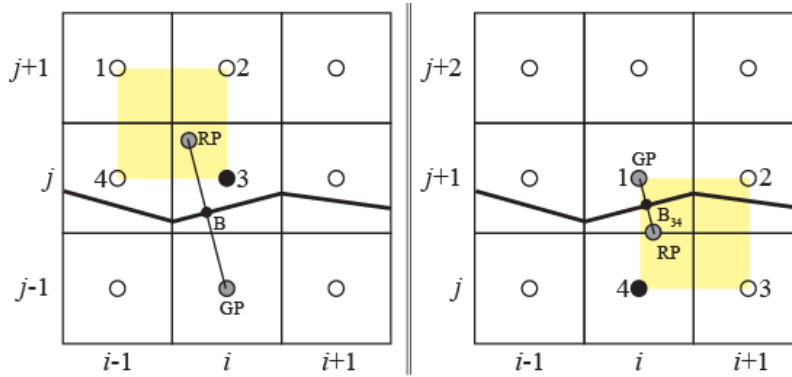


Figure 4. Procedure for determining the values of the variables in a ghost cell.

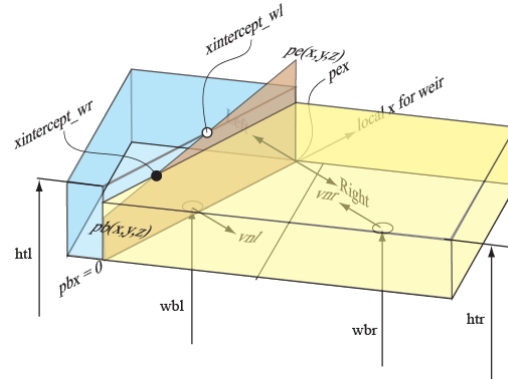


Figure 5. Definition sketch of a cut-cell boundary reach with overtopping.

Depending on the height of the cut-cell boundary and the water surface elevation on both sides, an overtopping discharge of q may be flowing from one side to the other. Figure 5 shows a cut-cell boundary reach with regions of unsubmerged flow, submerged flow and no flow. In order to be able to take into account all possible flow situations, the reach is divided into a number of equal-length sub-reaches. Using the ogee weir equation, the incremental overtopping discharge, Δq_j is separately calculated for each sub reach based on the elevation of the weir at the sub-reach center and the water depths on both sides. These incremental discharges are then summed up to determine the total discharge passing over the reach, q .

VALIDATION OF CUT-CELL BOUNDARY METHOD AND TEST CASES

Circular dam break in a closed square domain

The case of a 4m-diameter circular dam in a 15×15m close rectangular domain filled with 1m-deep still water is used to validate the cut-cell boundary method. Referring to Figure 6, the square domain for the reference case is defined along the grid lines by imposing a fully reflecting wall boundary condition. In the test case, the 15×15m square domain is defined inside a 25×25m domain by using cut-cell boundaries making an angle of 45° with the gridlines of the computational mesh. In both cases the computations are carried out with $\Delta x = \Delta y = 0.5m$ and $\Delta t = 0.1s$.

Computed water surface contours for both solutions are shown in Figure 7 for the first 5 seconds. The test-case solution is rotated 45° counter clockwise to facilitate comparison with the reference solution. The color-bar range is varied with time for better readability. However at each time, the test solution and the reference solution use the same color-bar range. As it can be seen, the water depth patterns obtained with cut-cell boundary method are almost identical to those of the reference solution.

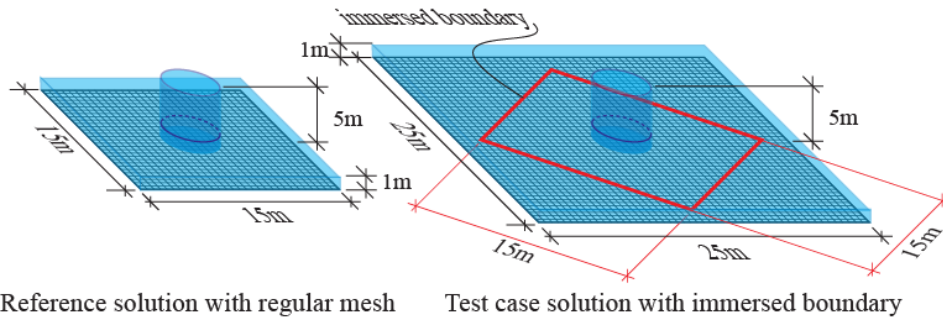


Figure 6. Set-up for circular dam break case with and without cut-cell boundary capability.

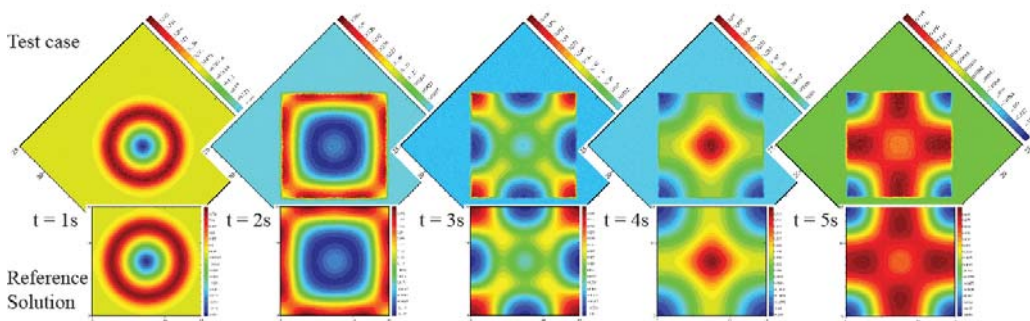


Figure 7. Circular dam break simulation with and without cut-cell boundary.

Dam-break flood over a variable height cut-cell boundary

Figure 8 shows the experimental set-up for this test case. The wedge shaped cut-cell boundary has a very low height near the apex. The height of the cut-cell

boundary increases towards both extremities. The dam located along the upper boundary of the computational domain breaks at the beginning of the simulation. Everywhere else there is still water with a depth of 0.5m.

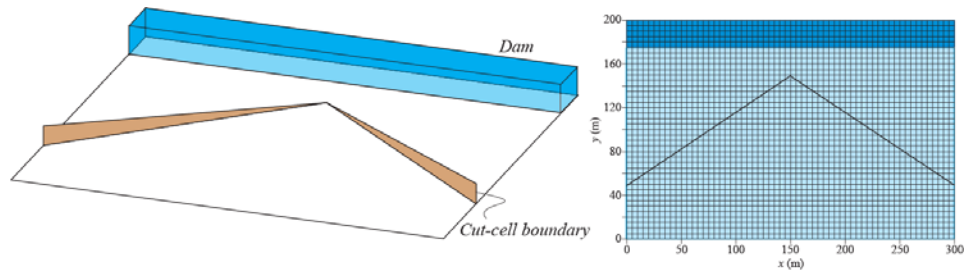


Figure 8. Set-up for dam-break flood over a variable-height cut-cell boundary.

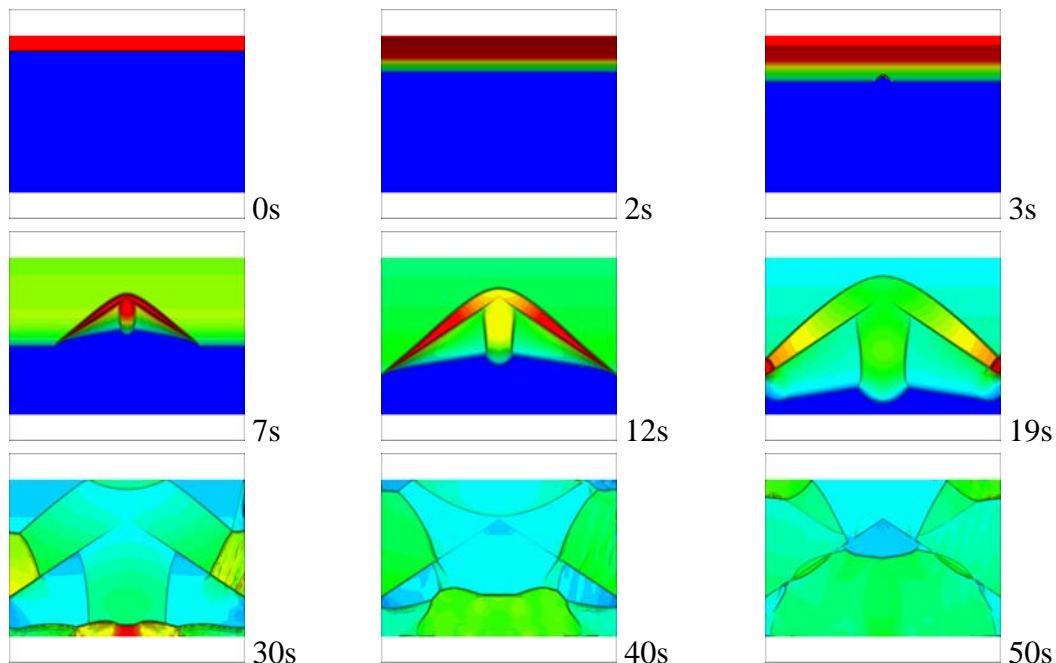


Figure 9. Water surface contours for dam-break flood over a variable-height cut-cell boundary. Numbers below the frames represent time in seconds.

Computed water-surface elevations are plotted in Figure 9 at different times after the dam break. When the dam-break flood reaches the cut-cell boundary, the flow partly overtops boundary (in the middle part); partly it is reflected, leading to the formation of a moving hydraulic jump. As more water arrives toward the cut-cell boundary, eventually the overtopping takes place over its entire length. The following images show the interaction of various wave fronts resulting from this complex configuration. Since four sides of the computational domain are declared as a fully reflecting wall boundary, mass conservation can be easily verified. Loss of mass at the end of several hundred seconds of simulation is found to be less than 1%.

CONCLUSIONS

The paper described the implementation of a two-sided cut-cell boundary method in the numerical model CCHE2D-FLOOD, which uses a first order upwinding finite-volume scheme to solve 2D shallow water equations on complex topography defined by a DEM. This two-sided cut-cell boundary method allows representing the linear terrain features on a Cartesian regular mesh, which cannot be adequately captured in a DEM. The implemented method allows overtopping of the cut-cell boundary. The results of two selected test cases demonstrate the effectiveness of the method.

REFERENCES

- Causon, D.M., Ingram, D.M., Mingham, C.G., Yang, G. and Pearson, R.V. (2000). "Calculation of Shallow Water Flows Using a Cartesian Cut Cell Approach." *Advances in Water Resources*, 23:545-562.
- Ghias, R., Mittal, R. and Dong, H. (2007). "A sharp interface immersed boundary method for compressible viscous flows." *J. Comput. Phys.*, 225, pp.528-553
- Helzel C., Berger M.J. and Leveque R.J. (2005). "A high-resolution rotated grid method for conservation laws with embedded geometries." *SIAM Journal on Scientific Computing*, vol. 26, no. 3, pp. 785-809.
- Miglio, E., Altinakar, M.S., and Tayfur, G. (2008). "Representation of Linear Terrain Features in 2D Free Surface Model using Cut-Cell Boundary Method." *Proc. Int. Conf. on Fluvial Hydraulics River Flow 2008*, 3-5 September 2008, Cesme, Turkey.
- Mittal, R. and Iaccarino, L. (2005). "Immersed Boundary Methods, Annual Review of Fluid Mechanics." Vol. 37: 239-261.
- Ying, X., Khan, A.A. and Wang, S.S.Y. (2003a). "An Upwind Method for One-Dimensional Dam Break Flows." *Proc. of 30th IAHR Congress*, pp. 245-252, Thessaloniki, Greece, August, 2003.
- Ying, X., Khan, A. A. and Wang, S.S.Y. (2004). "An Upwind Conservative Scheme for Saint-Venant Equations." *Journal of Hydraulic Engineering*. Vol.130, No.10, pp. 977-987, 2004.
- Ying, X. and Wang, S.S.Y. (2004). "Two-Dimensional Numerical Simulations of Malpasset Dam-Break Wave Propagation." *Proc. of 6th International Conference on Hydroscience and Engineering, Brisbane, Australia, Book of Abstracts*, pp.137-138, Manuscript on CDROM, May, 2004.
- Ying, X., Wang, S.Y. and Khan, A.A. (2003b). "Numerical Simulation of Flood Inundation Due to Dam and Levee Breach." *Proceedings of ASCE World Water & Environmental Resources Congress 2003 (CD-ROM)*, Philadelphia, USA, June 2003.